①

LECTURE 3

Boebinger

ABNORMAL NORMAL STATE of the HIGH-Tc's
(and WHY USE HIGH MAGNETIC FIELDS ?)

LOW - DIMENSIONAL TRANSPORT
and QUASI-PARTICLE CONFINEMENT

REVEALING QUANTUM CRITICAL POINTS
in the HIGH-Tc PHASE DIAGRAM

SCIENCE, Correlated Electron Systems, 21 April 2000
"Advances in the Physics of High-Temperature Superconductivity"
J. Orenstein and A.J. Millis, Science 288 (2000) 468
"Quantum Criticality: Competing Ground States in Low Dimensions"
Subir Sachdev, Science 288 (2000) 475
"Sources of Quantum Protection in High-Tc Superconductivity"
Philip W. Anderson, Science 288 (2000) 480

THE Theory of SUPERCONDUCTIVITY in the High-Tc Cuprates,
P.W. Anderson (Princeton Univ. Press, 1997) ISBN 0-691-04365-5

②

CHARGE MOTION (hard).   STRIPE MOTION (easy).

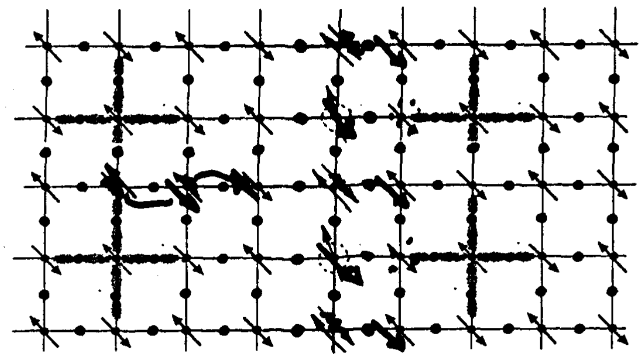

The PROs and CONs of CONFINEMENT

---Confinement might occur in the high-Tc cuprates, due to spin-charge separation.

For reviews, see P.A. Lee, Physica C 317-318 (1999) 194
and *THE Theory of SUPERCONDUCTIVITY in the High-Tc Cuprates*,
P.W. Anderson (Princeton Univ. Press, 1997) ISBN 0-691-04365-5

---There might be a more down-to-earth explanation.

By an accident of band structure, the interplane hopping matrix element vanishes at the nodal point ($\pi/2$, $\pi/2$).

If normal-state transport in underdoped cuprates is dominated by the Fermi arc near ($\pi/2$, $\pi/2$), then c-axis conductivity can be strongly suppressed.

For a review, see "Advances in the Physics of High-Temperature Superconductivity"
J. Orenstein and A.J. Millis, Science 288 (2000) 468

---Confinement might have been observed in double-layer quantum Hall systems.

"Confinement" in the One-Dimensional Hubbard Model:
Irrelevance of Single-Particle Hopping", Anderson, PRL (1991)
as reproduced in *THE Theory of SUPERCONDUCTIVITY in the High-Tc Cuprates*,
P.W. Anderson (Princeton Univ. Press, 1997) ISBN 0-691-04365-5

which cites G.S. Boebinger, et al, PRL **65** (1990) 235.

4

FRACTIONAL QUANTUM HALL EFFECT

J. P. Eisenstein and H.L. Stormer, Science **248** (1990) 1510

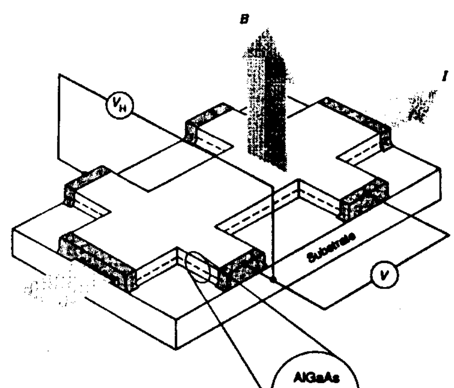

Fig. 1. A typical Hall bar sample. The structure is formed by chemically etching away unwanted material. The dotted line indicates the 2-D electron gas at the interface between gallium arsenide (GaAs) and aluminum gallium arsenide (AlGaAs). The magnetic field B and electrical current I are shown, as are the longitudinal and Hall voltages, V and V_H, respectively. The shaded regions at the ends of each arm of the bar are where electrical contact is made to the 2-D electron gas.

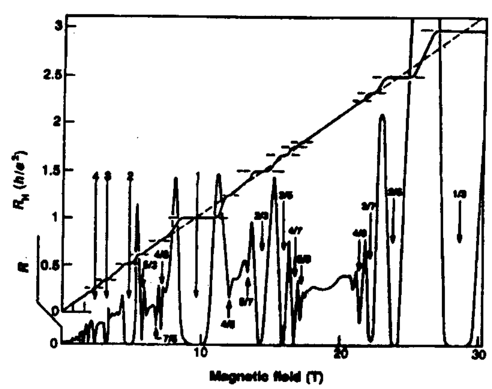

Fig. 2. Composite view showing the Hall resistance R_H and longitudinal resistance R of a 2-D electron gas versus magnetic field. The diagonal dashed line passing through the R_H trace represents the classically expected Hall resistance for this sample. For each of the plateaus in R_H there is an associated minimum in R. The numbers give the value of p/q determined from the value of R_H on the plateaus. While some of the p/q values are integers, the great majority are fractions. Note in particular the "1/3 state" at the far right. This most prominent example of the fractional quantum Hall effect exhibits a Hall plateau at $R_H = (h/e^2)/(1/3) = 3h/e^2$.

5

LANDAU LEVELS in a magnetic field

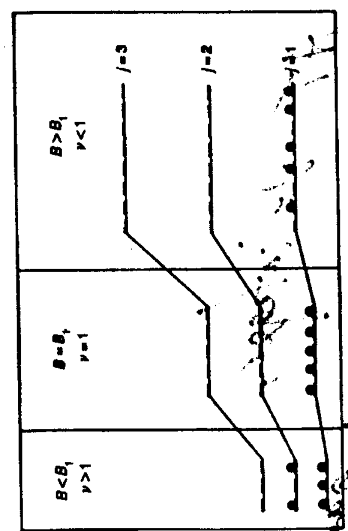

Fig. 3. Three lowest Landau levels, $j = 1,2,3$, in a five-electron system. Each panel corresponds to a specific magnetic field, B. The number of available states within each level is indicated. In the right-hand panel the magnetic field is high enough so that all five electrons may reside in the lowest level. In the middle panel the field has been reduced to the value B_1 where the lowest level is completely occupied and all higher levels are empty. This corresponds to the filling fraction $\nu = 1$. In the left panel the field has been further reduced, forcing some electrons into the $j = 2$ Landau level.

THE LAUGHLIN WAVEFUNCTION

$$\psi_m = \exp\left(-\tfrac{1}{4}\sum_l |z_l|^2\right)\left\{\prod_{j<k}(z_j - z_k)^m\right\}$$

PICTURES AT A
LAUGHLIN WAVEFUNCTION EXHIBITION

$\nu = 1 \qquad \psi_1 = \pi(z_i - z_j)^1$

$\nu = 1/3 \qquad \psi_3 = \pi(z_i - z_j)^3$

LAUGHLIN, PRL 50 ('83) 1395

9

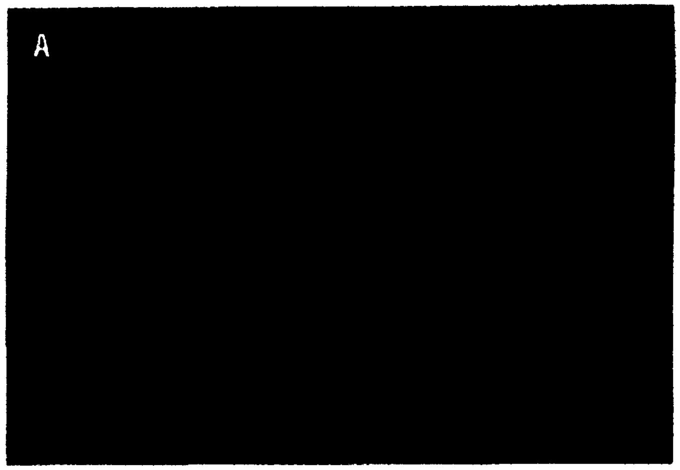

One electron in a magnetic field.
The minima occur because the electron wavefunction
picks up 2π phase shift in circulation around a flux line.

8

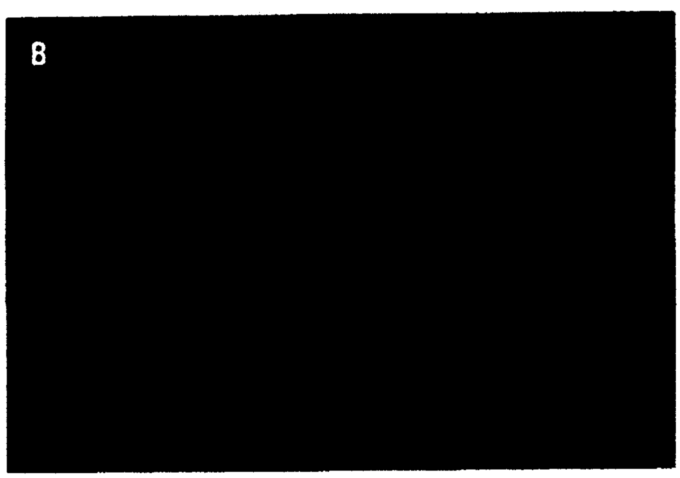

At Landau Level filling factor, $\nu = 1$.
The number of flux quanta equals the number of electrons.
The Slater determinant wavefunction is the $m = 1$ Laughlin wavefunction.
The $m = 1$ Laughlin wavefunction...
is odd under electron exchange.
picks up 2π phase shift when one electron circulates around another.

(11)

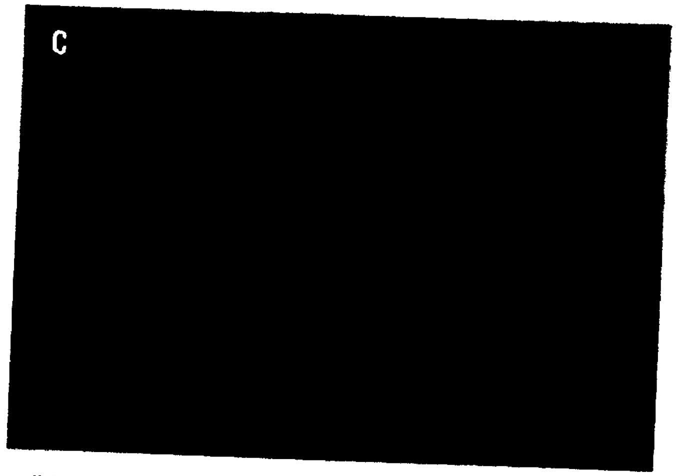

A possible configuration at Landau Level filling factor, $\nu = 1/3$.
The number of flux quanta is three times the number of electrons.
There are many equivalent permutations.
The avoidance of flux quanta positions not associated with an electron wastes energy.

(10)

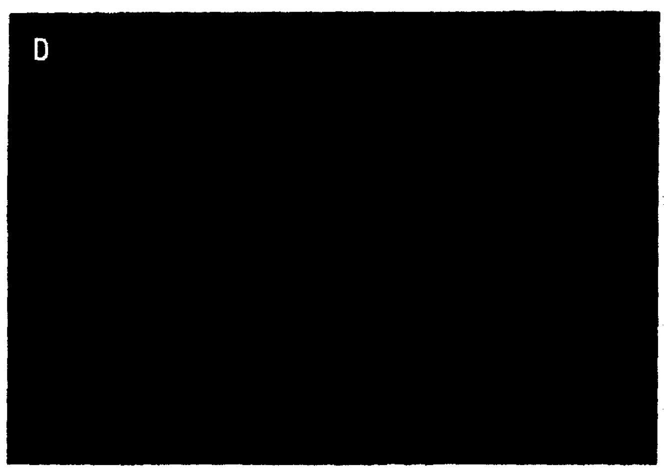

The Ground State at Landau Level filling factor, $\nu = 1/3$.
The number of flux quanta is three times the number of electrons.
The m = 3 Laughlin wavefunction...
is odd under electron exchange.
picks up 6π phase shift when one electron circulates around another.

13

One electron in a magnetic field

$\nu = 1$, one flux per electron

$\nu = 1/3$, three flux minima
for electron minimum

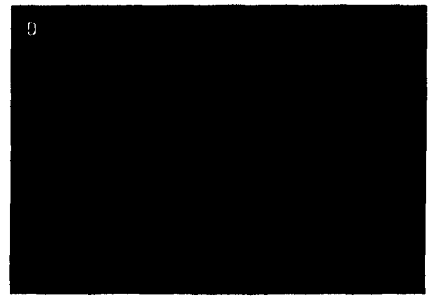

Ground state at $\nu = 1/3$,
three flux tied to each electron

J. P. Eisenstein and H.L. Stormer, Science **248** (1990) 1510

12

QUASIHOLES and QUASIPARTICLES at $\nu = 1/3$

To generate a quasihole or quasielectron at z_0, Laughlin employs raising and lowering operators representing the addition and removal of a single flux quantum from the system.

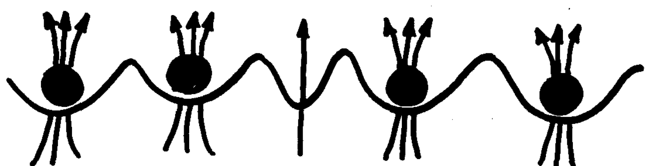

$$\left\{\prod_i (z_i - z_0)\right\}\left\{\prod_{j<k} (z_j - z_k)^3\right\}$$

A QUASIHOLE at $\nu = 1/3$....
is one extra flux quantum moving freely (which forms a first-order minimum).
is avoided by other electrons, yielding a local electric charge of (+1/3 e).

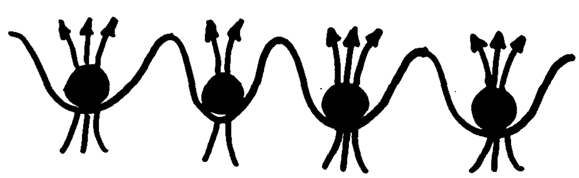

$$\left\{\prod_i \left(\frac{\partial}{\partial z_i} - \frac{z_0}{\ell_0^2}\right)\right\}\left\{\prod_{j<k} (z_j - z_k)^3\right\}$$

A QUASIPARTICLE at $\nu = 1/3$....
is a deficit of one flux quantum (one electron moving with only two flux quanta).
is avoided less by other electrons, yielding a local excess of 1/3 electrons (with a -1/3 e charge).

Laughlin, PRL **50** (1983) 1395.

DOUBLE QUANTUM WELLS

$n = 4 \times 10^{11}\ cm^{-2}$
(~160 Å BETWEEN e^-)

$\Delta_{SAS} = 4 - 17\,K$

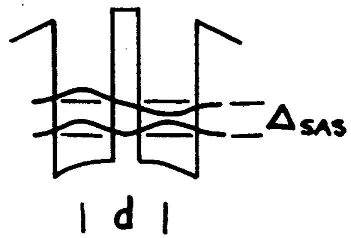

$d = 168 - 191$ Å

WELL WIDTHS	140 Å
BARRIER WIDTHS	28 - 51 Å

$$\ell = \sqrt{\frac{h}{eB}} = \frac{256}{\sqrt{B(T)}} \quad (\text{Å})$$

$$\frac{e^2}{\varepsilon \ell} = 51\sqrt{B(T)} \quad (K)$$

SINGLE ELECTRON ENERGY LEVELS

Three relevant single electron energies:

- Cyclotron energy, $\hbar\omega_c$
- Zeeman energy, $g^*\mu_B B_{total}$
- Symmetric-~~antisymmetric energy~~, Δ_{SAS}

$\nu = n_{2D}h/eB_\perp \longleftrightarrow$ number of occupied energy levels

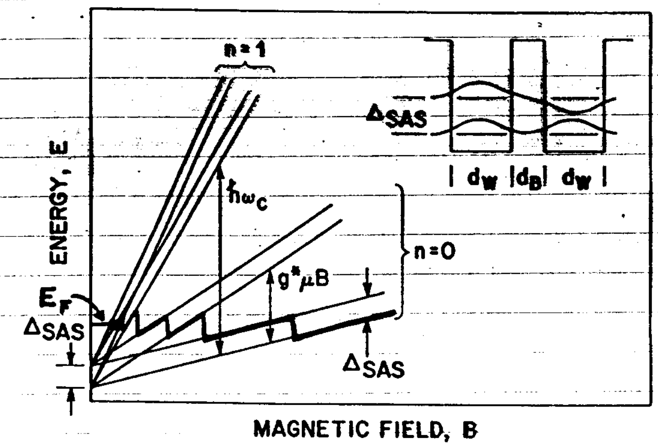

$\nu = 4n$	$\nu = 4n+2$	$\nu =$ ODD
$\hbar\omega_c$	$g^*\mu B$	Δ_{SAS}

AND ... 32% DENSITY INCREASE   19b/29

16

$d_B = 40$ Å SAMPLE

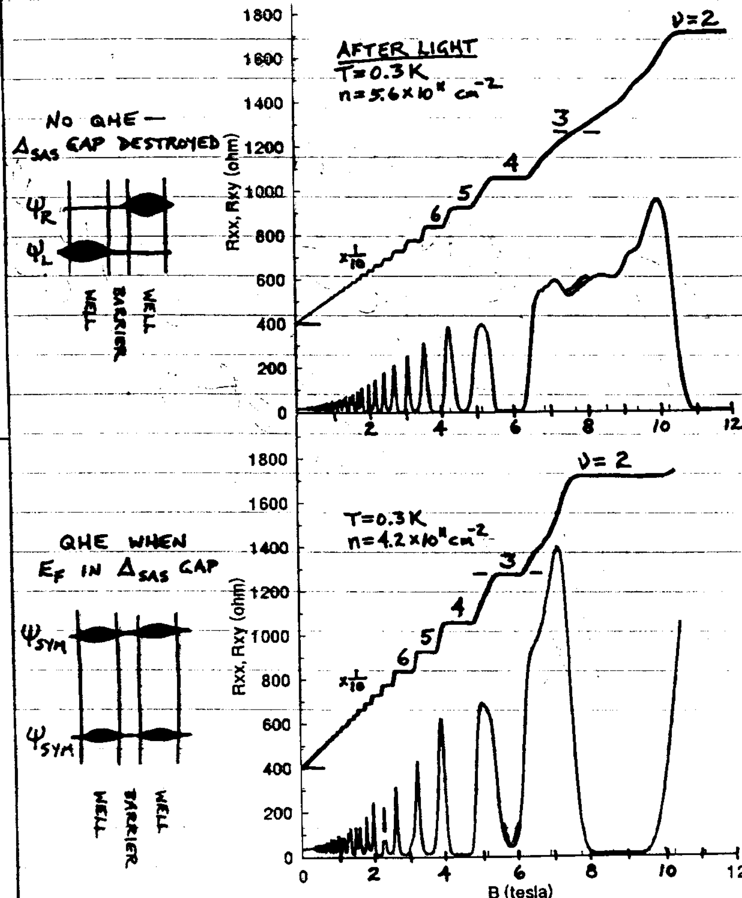

BOEBINGER et al PRB 45 (1992) 11,391 (RC)

AND 13

AT&T

E-9148 (6-85) AT&T BELL LABORATORIES

8

VG. NO.____

TOP
DO NOT AFFIX OVERLAYS ALONG THIS SURFACE

17

DOUBLE QUANTUM WELL
PHASE DIAGRAM AT ν=ODD

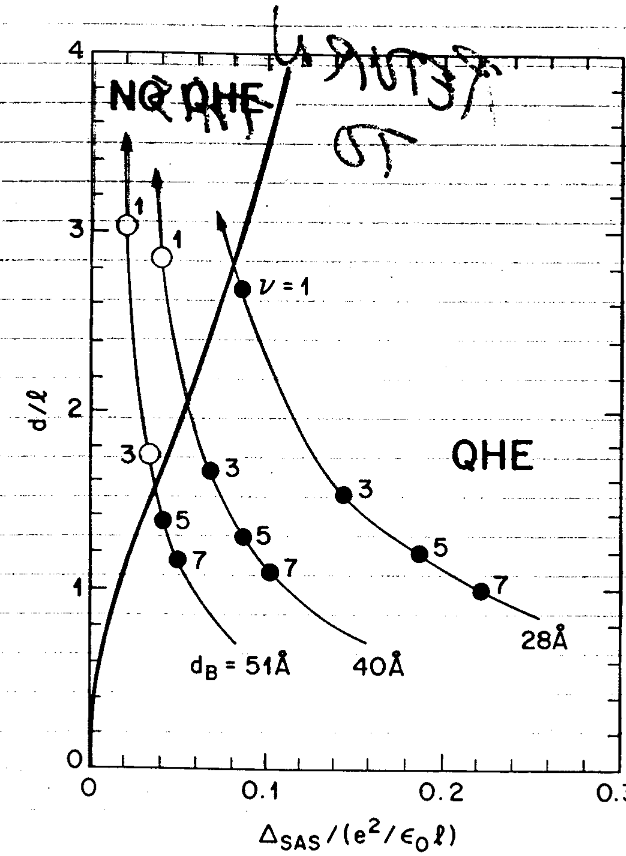

AT&T

E-9148 (6-85) AT&T BELL LABORATORIES

1/29

(18)

DESTRUCTION OF QUANTUM HALL STATES

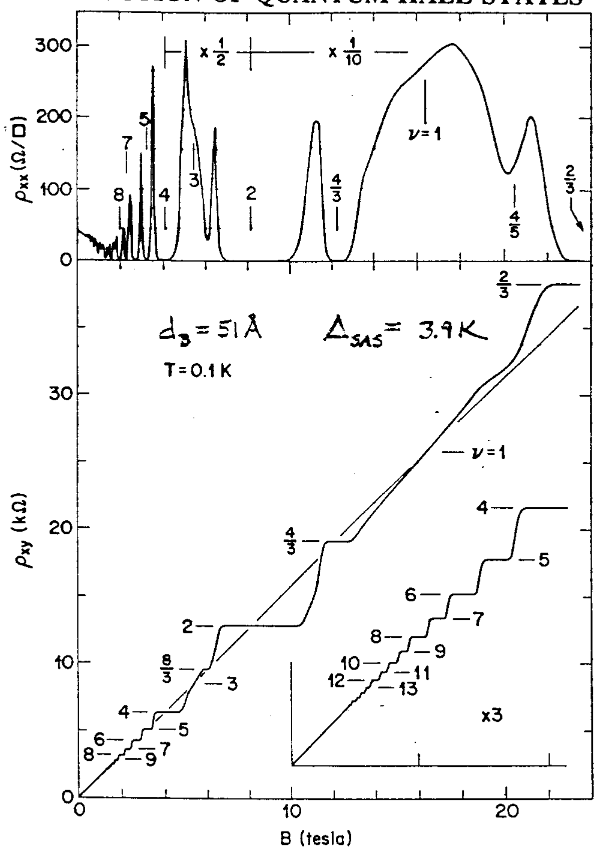

BOEBINGER et al PRL 64 (1990) 1793

SUMMARY OF THREE SAMPLES

d_B(Å)	Δ^{calc}_{SAS}(K)	Δ^{meas}_{SAS}(K)	missing states
28	17.3	17.5±0.5	—
40	8.1	7.7±0.5	ν = 1
51	3.9	—	ν = 1,3

7

(19)

(BALL AND STICK) MODEL INCLUDING TUNNELING

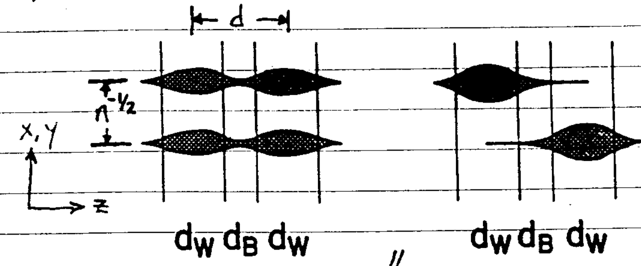

SINGLE e^- MODEL // DOMINANT N-N CORRELATIONS

CONFINEMENT ENERGY COST   COULOMB ENERGY GAIN

$$\Delta^{calc}_{SAS} \le \left(\frac{C_0 e^2}{\epsilon}\right)\left[\frac{1}{n_{eff}^{-1/2}} - \frac{1}{(n_{eff}^{-1}+d^2)^{1/2}}\right]$$

(SINGLE PARAMETER, C_0)

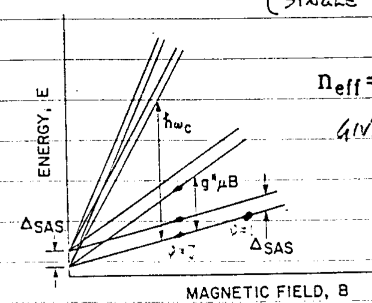

$n_{eff} = n_{2D}/\nu = eB_\perp/h.$

GIVES MAGNETIC FIELD DEPENDENCE

AT ν=1, n_{2D} ELECTRONS

AT ν=3, $n_{2D}/3$

etc.

MACDONALD, PLATZMAN, BOEBINGER, PRL 65 (1990) 775.

MOTT M-T TRANSITION

KE. vs P.E

12

START IN THIN BARRIER LIMIT

B=0 ↓ LIKE 2 LOWEST SUBBANDS

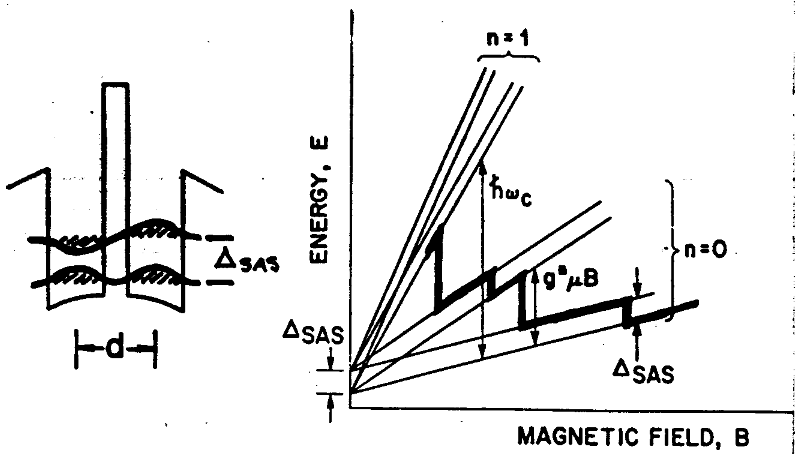

$\nu =$, 2 , , 4 , , 6 ....

$2/3$ $4/3$ ....

$2/5$ $4/5$ ....

LIMIT OF $d/\ell \to 0$ $d/\ell \to \infty$

≈1 IS TUNNELING GAP

THEORETICAL APPROACHES to the HIGH-Tc CUPRATES

discussion from "Singular Quasiparticle Scattering in the Proximity of Charge Instabilities"
C. Castellani, C. Di Castro, and M. Grilli, PRL **75** (1995) 4650

--- Low dimensionality and correlations break down the Fermi liquid.

---Formation of a two-dimensional Luttinger liquid. (Anderson)

--- Landau Fermi liquids serve as a suitable starting point for theory and abnormal normal state arises from strong scattering processes at low energy between the quasiparticles.

QCP **---Magnetic scattering in a *nearly antiferromagnetic Fermi liquid* is responsible for abnormal normal state and superconducting pairing.**
Monthoux and Pines, Phys. Rev. B47 (1993) 6069

QCP **---Excitonic scattering leads to *marginal Fermi liquid behavior.***
Varma, PRL 75 (1995) 898

---Singular scattering by gauge fields, arising from implementing the *resonating-valence-bond* theory in the *t-J* model.
Nagaosa and Lee, PRL 64 (1990) 2450; Phys. Rev. B46 (1992) 5621

QCP **---Long-range Coulomb interactions near a charge instability (stripe formation) give rise to singular scattering**
Castellani, Di Castro, and Grilli, PRL 75 (1995) 4650

21

QUANTUM CRITICAL POINT in the HIGH-Tc CUPRATES

--- In the quantum critical region, temperature is the only energy scale controlling the physics.
--- Strong critical fluctuations can mediate singular interactions between quasiparticles.
--- These singular interactions can provide both a strong pairing mechanism and a source of non-Fermi liquid behavior.

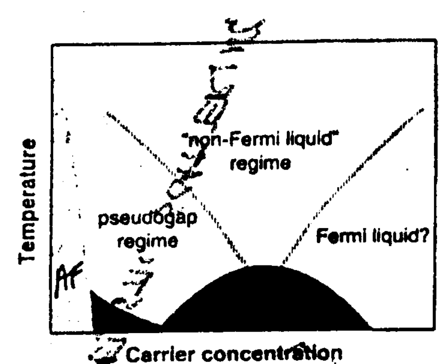

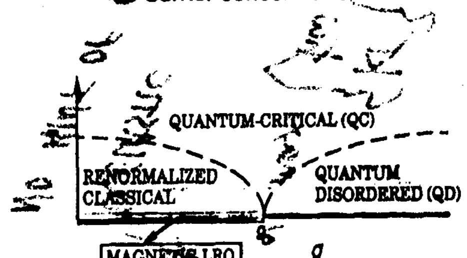

FIG. 1. Phase diagram of $\mathcal{H}$ (after Ref. [4]). The magnetic LRO can be either spin-glass or Néel type, and is present only at $T=0$. The boundaries of the QC region are $T \sim |g-g_c|^{\nu}$.

22

SCALE-LESS and FEATURE-LESS SCATTERING RATE

dc resistivity

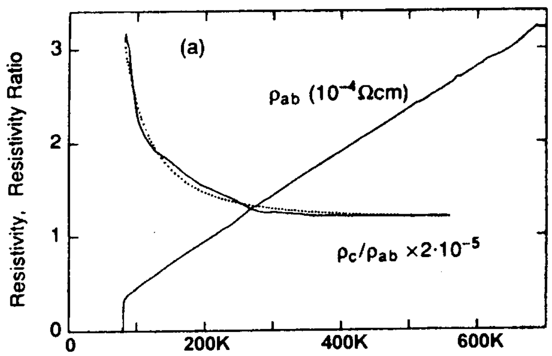

Figure 3.2b. Planar resistivity vs. T for a variety of materials. (b) Anisotropic resistivity of BISCO.

Optimally-doped Bi-2212, Martin, et al

optical conductivity

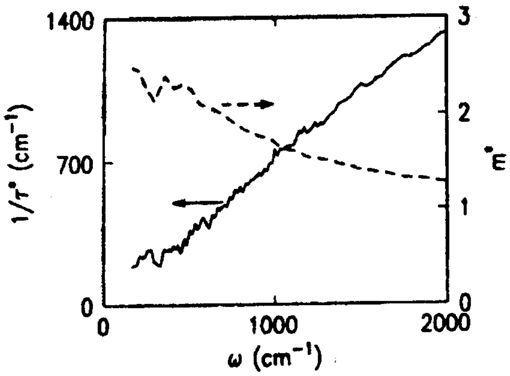

Optimally-doped YBCO, Schlesinger, et al

$$\frac{\hbar}{\tau} \sim \max\left\{\begin{matrix} kT \\ \hbar\omega \end{matrix}\right\}$$

$\tau \sim \tau_{INELASTIC}$

NO HINT OF ELASTIC SCATTERING

23

QUANTUM CRITICAL POINT in the HIGH-Tc CUPRATES

from "Universal Quantum-Critical Dynamics of Two-Dimensional Antiferromagnets"
Subir Sachdev and Jinwu Ye, PRL **69** (1992) 2411
[Ref 4 is Chakravarty, Halperin and Nelson, PRL **60** (1988) 1057; PR **B39** (1989) 2344]

--- A remarkable feature of the measured dynamic susceptibilities of the cuprates is that the frequency scale of the spin excitation spectrum is given simply by the absolute temperature *(ie. independent of all microscopic energy scales, such as an antiferromagnetic exchange constant).*

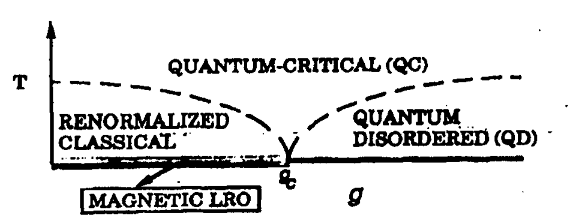

FIG. 1. Phase diagram of $\mathcal{H}$ (after Ref. [4]). The magnetic LRO can be either spin-glass or Néel type, and is present only at $T=0$. The boundaries of the QC region are $T \sim |g-g_c|^{z\nu}$.

---This is a very general property of finite-T quantum-critical spin fluctuations
---The coupling constant, g, depends on the ratios of Jij in *H*.
---At g_c, the correlation length diverges with exponent ν, $\varepsilon \sim |g-g_c|^{-\nu}$.
---At finite T, the thermal length, $\varepsilon_T \sim T^{-1/z}$, is the scale at which deviations from T=0 behavior are first felt.

---The Quantum Critical (QC) regime is defined by the inequality $\varepsilon_T < \varepsilon$
---In the QC regime, the spin system notices the finite value of T *before* becoming sensitive to the deviation of g from g_c.
---In the QC regime, dynamic spin correlations will be found to be remarkably universal.

24

QUANTUM CRITICAL POINT in the HIGH-Tc CUPRATES

from "Stripe Formation: A Quantum Critical Point for Cuprate Superconductors"
C. Castellani, C. Di Castro, and M. Grilli, J. Phys. Chem. Solids **59** (1998) 1694

--- There is a Quantum Critical Point related to local charge segregation (stripe phase) near optimum doping.
--- Superconductivity is a stabilizing mechanism against fully-developed charge ordering.

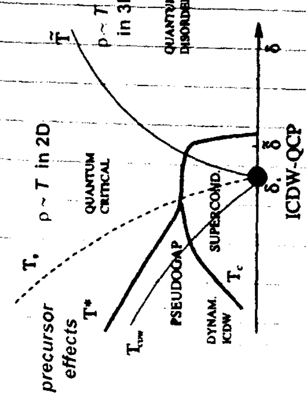

Fig. 1. Schematic structure of the temperature versus doping δ phase diagram around the ICDW-QCP. On the right, $T < \tilde{T}$: QD region [$\xi^{-2} \sim (\delta - \delta_c)$]; in the middle, $T > T_0$, $\tilde{T}$: QC (classical Gaussian) region $\xi^{-2} \sim T$]; on the left, $T < T_{CDW}$: "ordered" ICDW phase. The heavy line indicates the region of local (pseudogap) or coherent (superconducting) pairing. In the presence of pairing, i.e. for $T < T^*$, the ICDW "order" is purely dynamical.

EVIDENCE CITED
--- Resistivity
--- Neutron scattering
--- Hall number
--- Uniform susceptibility

see discussion and references in:
C. Castellani, C. Di Castro, and M. Grilli
Z. Phys. B103 (1997) 137.

INSULATOR--TO--METAL CROSSOVER IN THE NORMAL STATE OF A HIGH-Tc SUPERCONDUCTOR

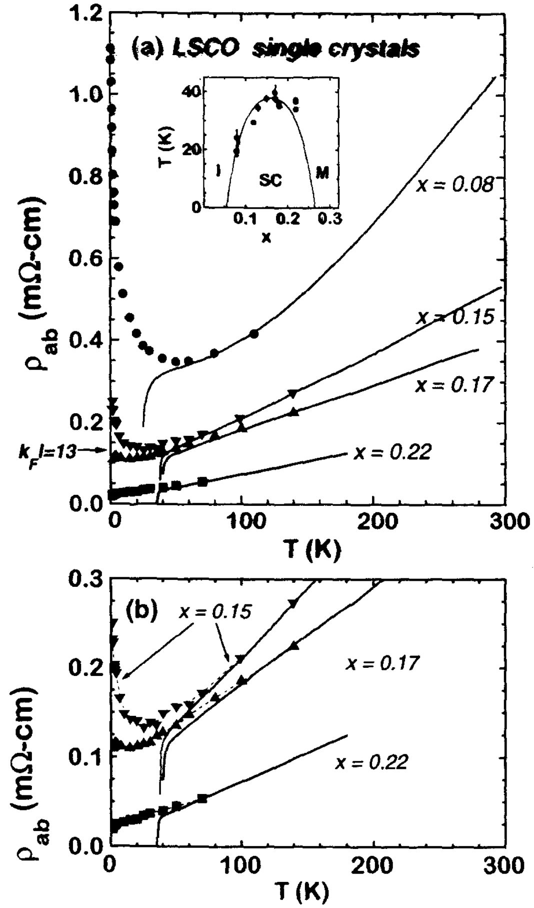

Boebinger, et al. PRL 77, 5417 (1996)

27

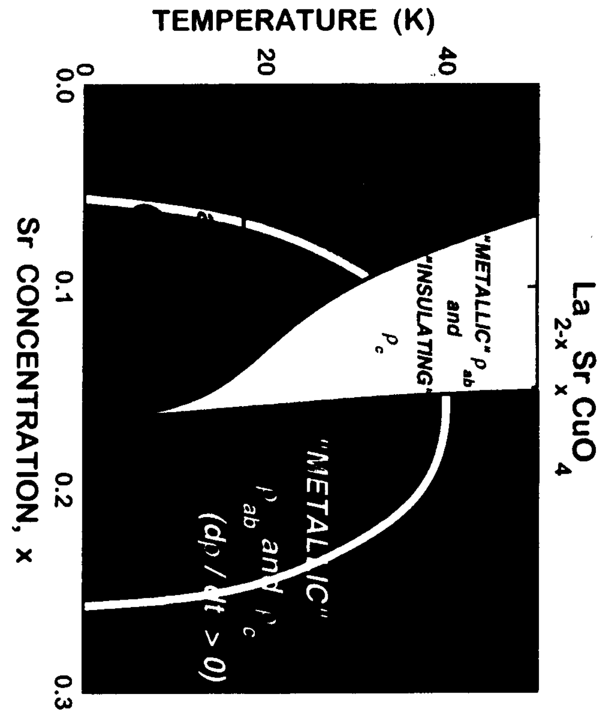

Insulator-Metal Crossover near Optimal Doping in $Pr_{2-x}Ce_xCuO_4$

(an electron-doped high-Tc cuprate)

Fournier, Mohanty, Maiser, Darzens, Venkatesan, Lobb, Czjzek, Webb, Greene
PRL **81** (1998) 4720

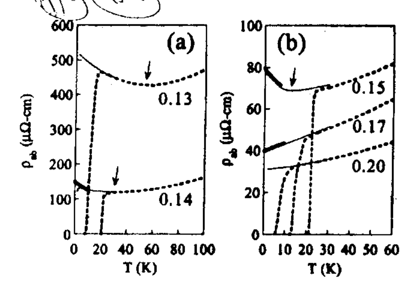

FIG. 1. Resistivity ρ_{ab} as a function of temperature for the c-axis oriented $Pr_{2-x}Ce_xCuO_4$ thin films in magnetic fields of 0 T (dashed lines), 8.7 T (thin lines), and 12 T (thick lines). (a) $x = 0.13$ and 0.14; (b) $x \geq 0.15$. The field is applied along the c axis.

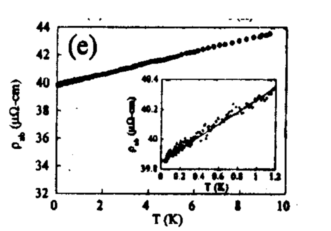

FIG. 2. ρ_{ab} below 10 K and at 12 T for some samples of Fig. 1: (a) and (b) $x = 0.14$; (c) and (d) $x = 0.15$; and (e) $x = 0.17$. In (e), the inset shows a magnified view of the subkelvin range.

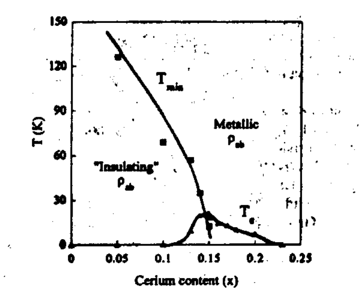

FIG. 3. Phase diagram determined from resistivity data of $Pr_{2-x}Ce_xCuO_4$ thin films. Solid triangles and solid squares are T_c and T_{min} (defined in text), respectively. The solid lines are guides to the eye.

28

29

Metal-Insulator Crossover in the Low-Temperature Normal State of $Bi_2Sr_{2-x}La_xCuO_{6+\delta}$

PRL 85 (2000) 638

S. Ono[1], Yoichi Ando[1,2], T. Murayama[1,2]
F.F. Balakirev[3], J.B. Betts[3], G.S. Boebinger[3]

[1] Central Research Institute of Electric Power Industry, Tokyo, Japan
[2] Dept. of Physics, Science University of Tokyo, Japan
[3] National High Magnetic Field Laboratory, Los Alamos National Laboratory, Los Alamos, New Mexico

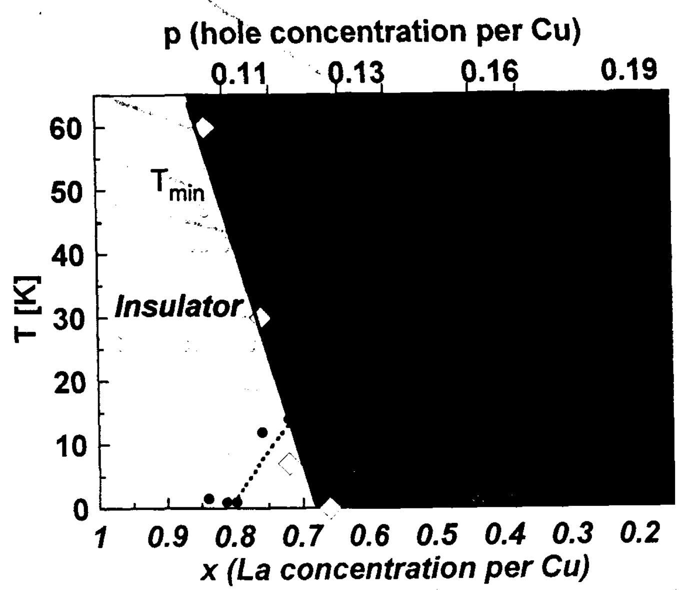

30

$Bi_2Sr_{2-x}La_xCuO_{6+\delta}$ Single Crystals

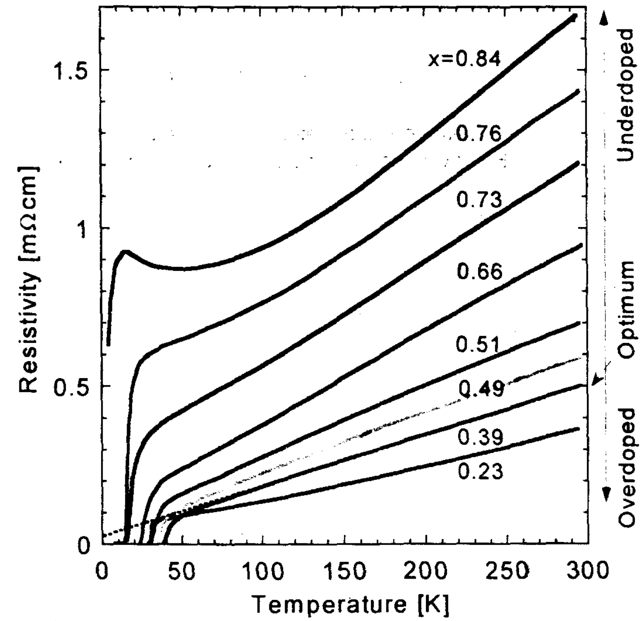

Samples grown at
Central Research Institute of Electric Power Industry, Tokyo, Japan

31

60 Tesla Pulsed Magnetic Fields

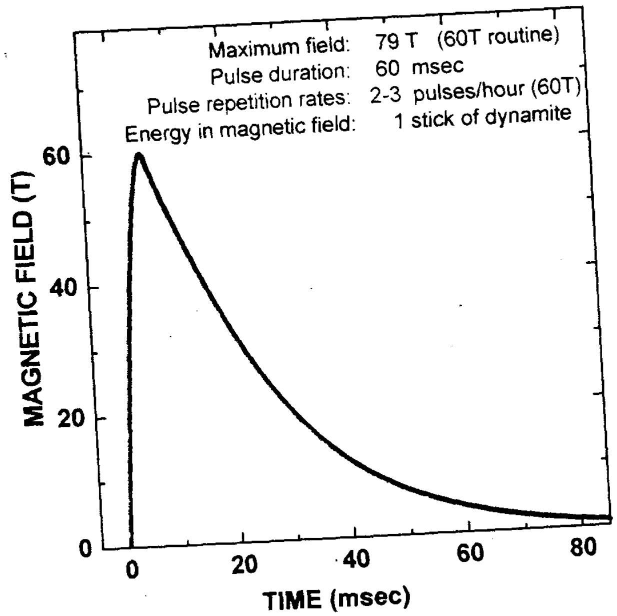

Magnetic fields at
National High Magnetic Field Laboratory,
Los Alamos National Laboratory, Los Alamos, New Mexico

32

Suppressing Superconductivity

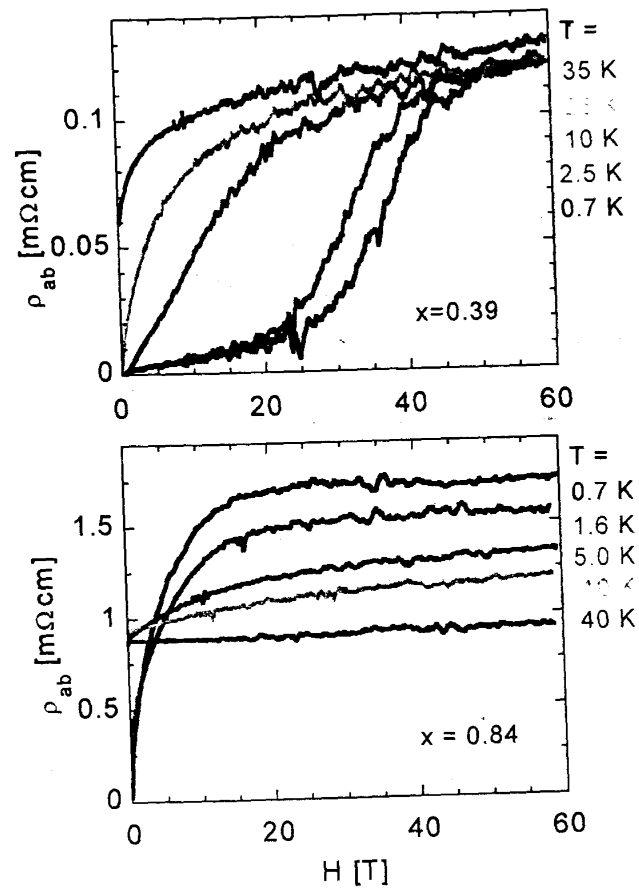

(33)

Revealing the Low-Temperature Normal State

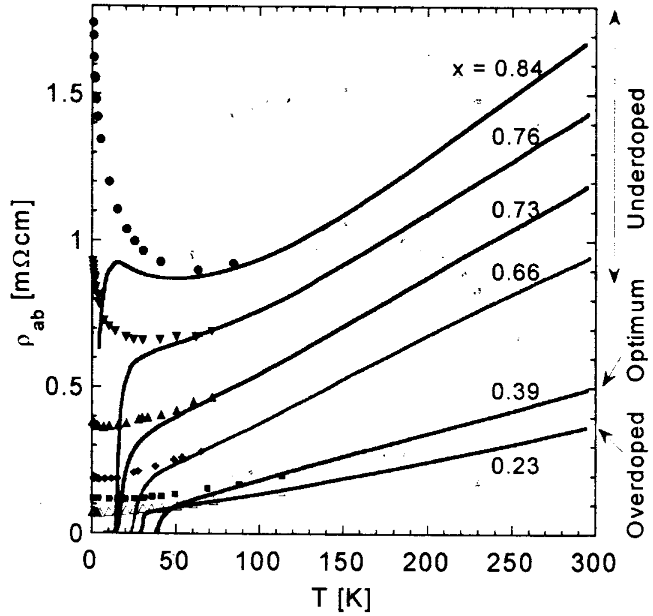

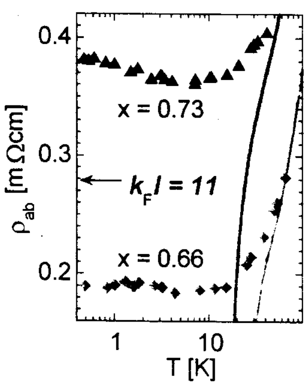

Close-up of the Crossover from Insulating Behavior to Metallic Behavior

$$\rho_{ab}/c_o = h/(e^2 k_F l)$$

(34)

Estimating Hole Concentration in $Bi_2Sr_{2-x}La_xCuO_{6+\delta}$

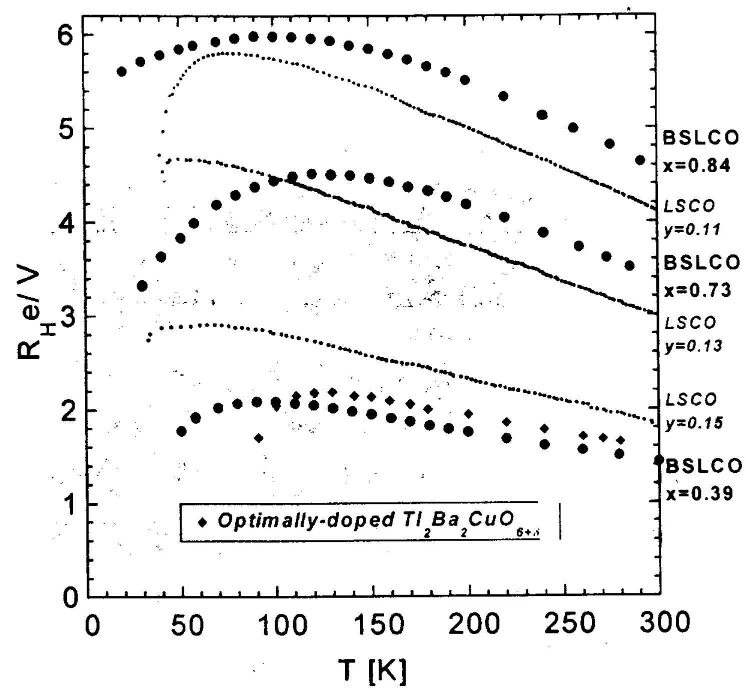

Similar Hall data for optimally-doped BSLCO, LSCO, Tl-2201.

Estimate BSLCO hole concentration by comparing with LSCO.

35

Proposed $Bi_2Sr_{2-x}La_xCuO_{6+\delta}$ Phase Diagram

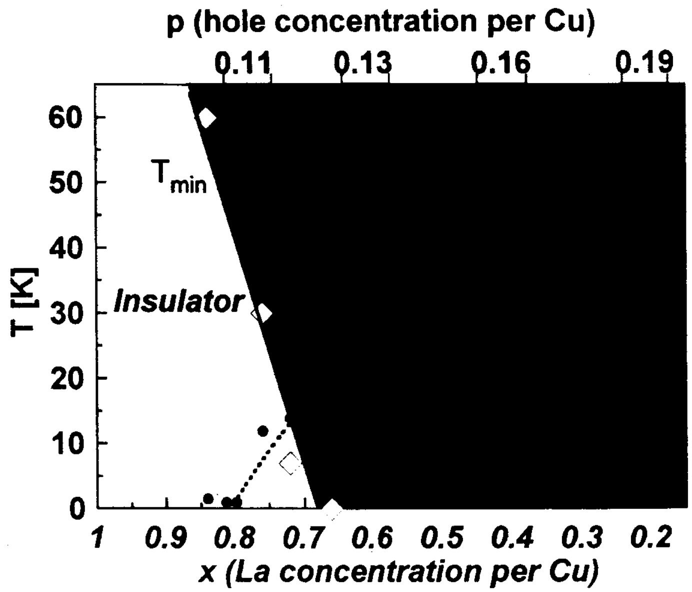

Insulator-to-Metal Crossover in BSLCO in underdoped regime.

36

Conclusions:

Metal-Insulator Crossover in the Low-Temperature Normal State
---occurs near p=1/8 in $Bi_2Sr_{2-x}La_xCuO_{6+\delta}$
---occurs near optimum doping in $La_{2-x}Sr_xCuO_4$

Similarities *between BSLCO and LSCO:*
Insulator-to-Metal Crossover
---observed when superconductivity is suppressed.
---occurs at relatively low normalized resistivities, $k_F l$ ~15.
Insulating Behavior exhibits Log-T divergence.

Differences *between BSLCO and LSCO:*
Insulator-to-Metal Crossover occurs gradually in BSLCO.
BSLCO data suggest the underdoped regime contains
a metallic state exhibiting unusual localization behavior.

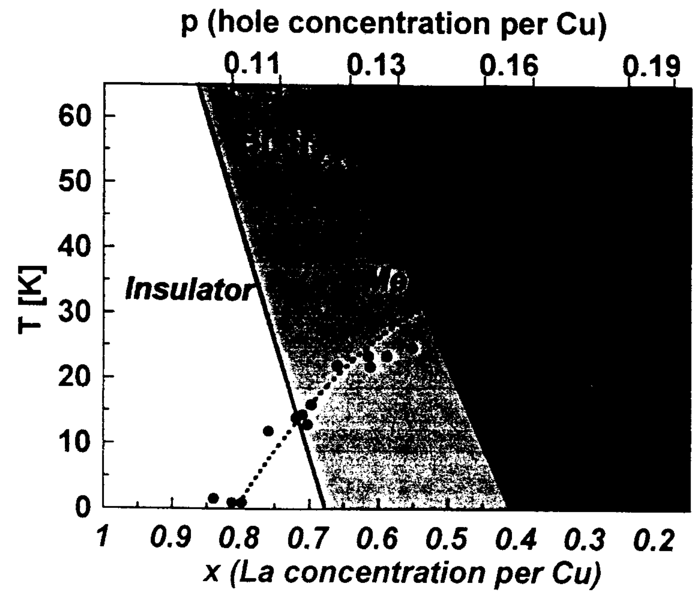

(38)

NHMFL Pulsed Magnet Facility in Los Alamos

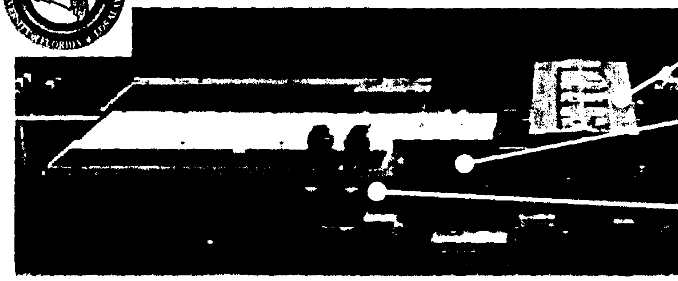

Generator Building

Long-Pulse Magnet Building

New Experimental Hall

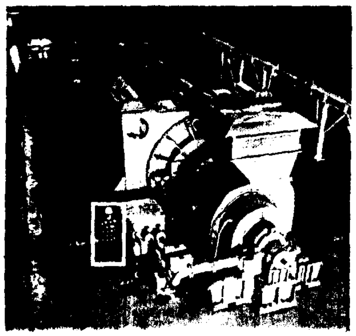

1.4 GVA Generator (man in foreground)

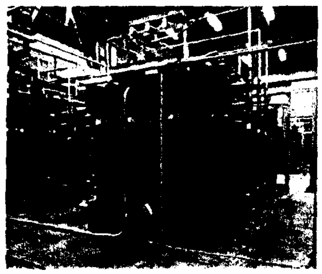

Seven 84 MVA Pulse-Shaping Power Supplies

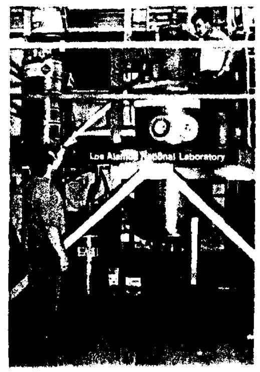

60T Long-Pulse Magnet

(37)

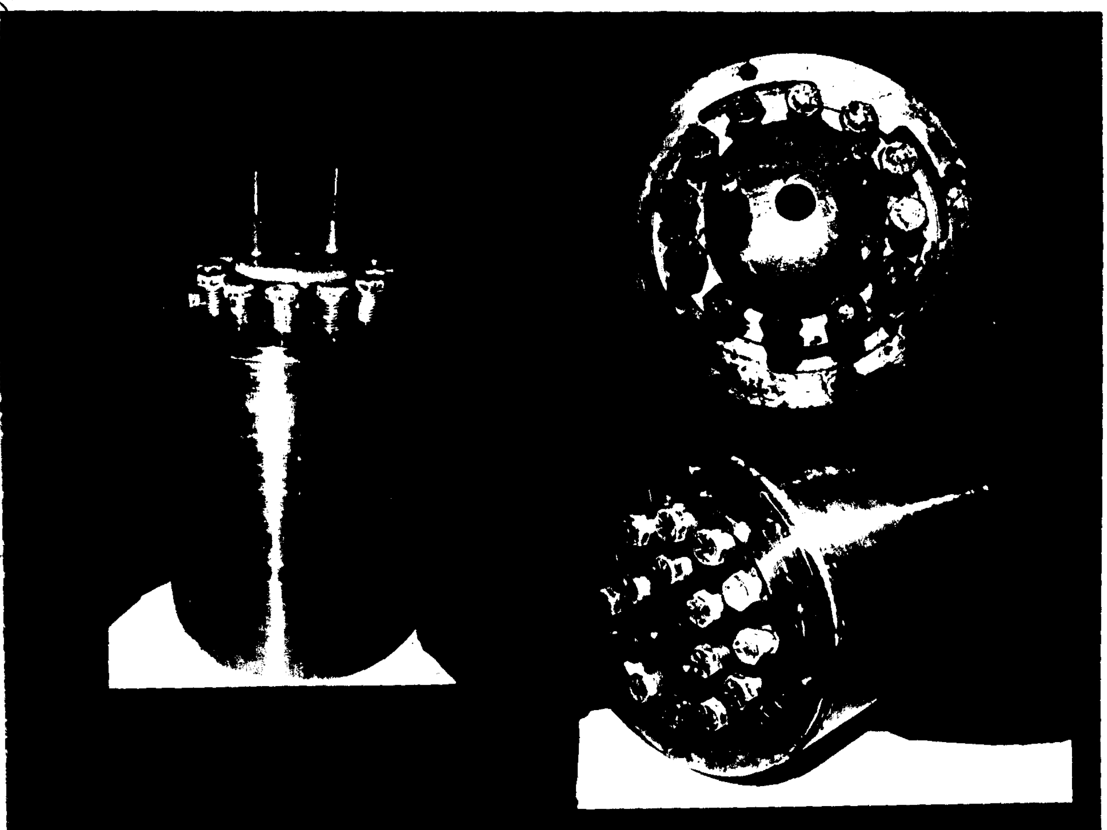

100 T Non-Destructive Magnet: Design and Materials

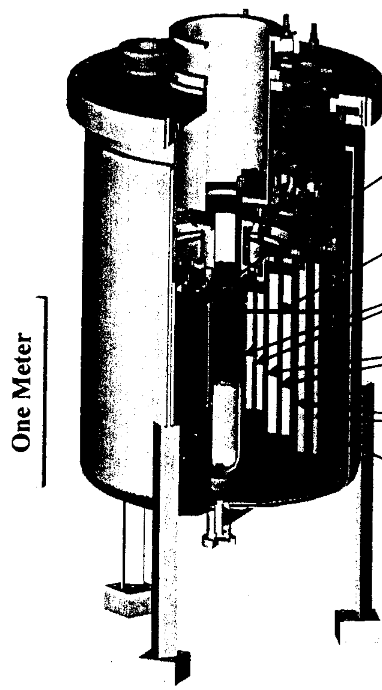

Insert Coil
(National Science Foundation)
CuNb Conductor
MP35N Alloy and Zylon Fiber Reinforcement

Outer Coil Set
(Department of Energy)

Coils 1 and 2
AL-60 (not CuAg or SS Clad) Conductor
301 SS Sheet Reinforcement

Coils 3 and 4
AL-15 Conductor
301 SS Sheet Reinforcement

Coils 5 and 6
AL-15 Conductor
Nitronic-40 Monolithic Reinforcement

Coil 7
Hard Cu Conductor
304 SS Monolithic Reinforcement

39

Simulated 100T pulse from the 100T Non-Destructive Magnet

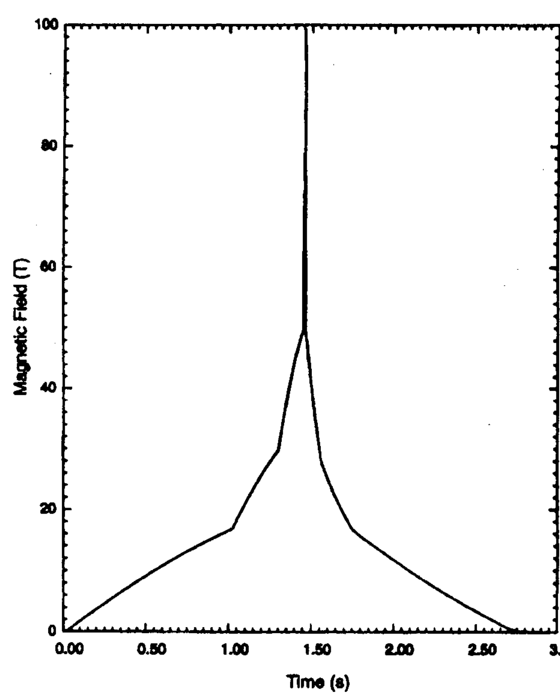

40